

Edge states of Spin-1/2 Two-Leg Ladder with Four-Spin Ring Exchange

Mitsuhiro Arikawa,¹ Shou Tanaya,¹ Isao Maruyama,² and Yasuhiro Hatsugai^{*1,3}

¹*Institute of Physics, University of Tsukuba 1-1-1 Tennodai, Tsukuba Ibaraki 305-8571, Japan*

²*Graduate School of Engineering Science, Osaka University,
1-3 Machikaneyama-cho, Toyonaka, Osaka 560-8531, Japan*

³*Kavli Institute for Theoretical Physics, University of California, Santa Barbara, California 93106, USA*

(Dated: October 30, 2018)

A topological insulator and its spin analog as a gapped spin liquid have characteristic low energy excitations (edge states) within the gap when the systems have boundaries. This is the bulk-edge correspondence, which implies that the edge states themselves characterize the gapped bulk spin liquid. Based on the general principle, we analyzed the vector chirality and rung singlet phases of the spin- $\frac{1}{2}$ ladder with ring exchange by using the edge states and the entanglement entropy.

PACS numbers: 73.43.Nq,75.10.Jm,75.40.Cx

I. INTRODUCTION

Spontaneous symmetry breaking has been fundamental to characterize phases of matter. An example is a magnetic phase where a local order parameter is defined as a quantum or thermal average of local combination of spins. Its ordered phase is not invariant against the symmetry operation which leaves the Hamiltonian invariant. In spite of enormous success of this concept, it has been also realized that there still exist many important phases that cannot be captured by the spontaneous symmetry breaking. Strong quantum fluctuation in low dimensions prevents such formation of the ordered state and makes it possible to realize states without any fundamental symmetry breaking. Such phases form a novel class of matter as quantum liquids and spin liquids. Typical examples of the quantum liquids are many of integer and fractional quantum Hall states. Spin analog of the quantum liquids is the spin liquid which includes the Haldane integer spin chain^{1,2}, generic valence bond solid (VBS) states^{3,4}, and some of the exactly solvable models that also have these spin liquid ground states (Kitaev model⁵, tensor category⁶ and so on).

As for an excitation of a quantum system, local characters of the order parameter and the symmetry breaking are fundamental. Generically speaking, one requires some mechanisms to have a gapless excitation. Typical machineries are the existence of the Fermi surface (formed by fermionic quasiparticles) and the Nambu-Goldston bosons associated with the broken continuous symmetry. An example of the latter is the spin wave excitation associated with the Neel order. Generically one may construct a gapless excitation by spatial modulation of the local order parameter such as the Lieb-Shultz-Mattis type spin twists⁷. In contrast, as for the quantum liquids and the spin liquids, it is natural to have a finite excitation gap unless one assumes exotic spinon

Fermi surfaces.

To characterize such quantum liquids and the spin liquids, topological quantities such as the Berry phases and the Chern numbers are quite useful^{8,9}. They do not have any symmetry breaking nor local order parameter. Still, there are many kinds of interesting quantum states without characteristic low energy excitation. Such non-trivial quantum phases are the topological insulator and its spin analog. A generic concept to discuss such a phase is the topological order which was first considered for the quantum Hall states¹⁰. As in the quantum Hall states^{11,12,13,14}, non-trivial topological insulators do have characteristic edge states or impurity states. The bulk is gapped and insulating. However the existence of boundaries or impurities brings low energy excitations. The quantum Hall state of graphene also belongs to this topological insulator^{15,16,17}. This is the bulk-edge correspondence where topologically non-trivial bulk guarantees the existence of localized modes and such low energy localized excitations characterize the gapped bulk insulator¹³ conversely.

Not only in the electronic systems, but also, in a quantum spin system such as the Haldane spin chain, is the bulk-edge correspondence realized as the existence of the Kennedy triplet for an open chain¹⁸, which was confirmed experimentally as well¹⁹. As a novel theoretical tool, the entanglement entropy (E.E.) for the gapped topological insulators has been quite successful to classify the VBS states of the spin chains^{4,20}, where this bulk-edge correspondence plays a fundamental role.

The spin- $\frac{1}{2}$ two-leg ladder with four-spin ring exchange has rich phase structure due to the frustration²¹. For this model, the static and dynamical properties have been intensively studied^{21,22,23,24,25,26,27,28,29}. Although the ring exchange model is simple, due to the frustration, the ground state is quite involved, namely in the vector-chirality (VC) phase. In this paper we consider the VC phase and the rung-single (RS) phase of this model to identify the ground state properties from the view point of the bulk-edge correspondence.

*corresponding author

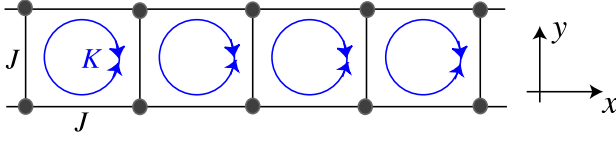


FIG. 1: Lattice structure: J is the exchange interaction in the leg or rung direction and K is the four-spin cyclic interaction. x -(y -) axis is defined as the leg (rung) direction.

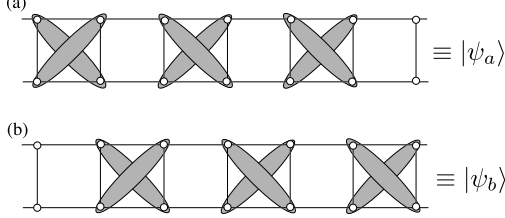


FIG. 2: Two types of the dimerized plaquette-singlets states. Shaded links denote the singlet of the two $S = 1/2$ spins.

II. MODEL

The Hamiltonian is given by

$$\mathcal{H}_{\text{cyc}} = J \left[\sum_{x=1}^{N/2} \sum_{y=1,2} \mathbf{S}_{x,y} \cdot \mathbf{S}_{x+1,y} + \sum_{x=1}^{N/2} \mathbf{S}_{x,1} \cdot \mathbf{S}_{x,2} \right] + K \sum_{x=1}^{N/2} (P_x + P_x^{-1}). \quad (1)$$

Hereafter, we parametrize the exchange parameter (J, K) as $(J, K) = (\cos \theta, \sin \theta)$. The four spin cyclic exchange consists of the two and four spin exchange interactions as²²,

$$P_x + P_x^{-1} = \mathbf{S}_{x,1} \cdot \mathbf{S}_{x,2} + \mathbf{S}_{x+1,1} \cdot \mathbf{S}_{x+1,2} + \mathbf{S}_{x,1} \cdot \mathbf{S}_{x+1,1} + \mathbf{S}_{x,2} \cdot \mathbf{S}_{x+1,2} + \mathbf{S}_{x,1} \cdot \mathbf{S}_{x+1,2} + \mathbf{S}_{x,2} \cdot \mathbf{S}_{x+1,1} + 4(\mathbf{S}_{x,1} \cdot \mathbf{S}_{x+1,1})(\mathbf{S}_{x+1,1} \cdot \mathbf{S}_{x+1,2}) + 4(\mathbf{S}_{x,1} \cdot \mathbf{S}_{x+1,1})(\mathbf{S}_{x,2} \cdot \mathbf{S}_{x+1,2}) - 4(\mathbf{S}_{x,1} \cdot \mathbf{S}_{x+1,2})(\mathbf{S}_{x,2} \cdot \mathbf{S}_{x+1,1}) + 1/4. \quad (2)$$

Here, $\mathbf{S}_{x,y}$ denotes a spin- $\frac{1}{2}$ operator at site (x, y) (see Fig. 1). We assume the system-size N to be even.

III. EDGE STATES

The Berry phases as topological order parameters classify the rung-singlet and the VC and RS phases of the model²⁹.

In the VC phase, Hamiltonian (1) is adiabatically connected to a decoupled vector-chiral model $\mathcal{H}_{\text{dvc}} = \sum_{x=\text{even}} (\mathbf{S}_{x,1} \times \mathbf{S}_{x,2}) \cdot (\mathbf{S}_{x+1,1} \times \mathbf{S}_{x+1,2})$, whose ground

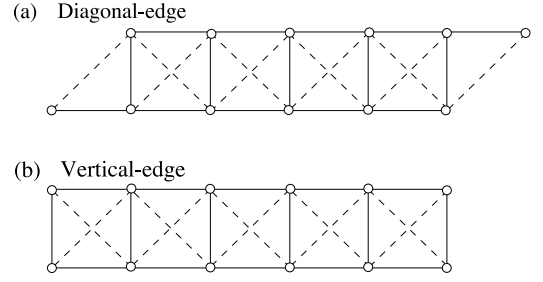


FIG. 3: Two types of open boundary conditions (OBCs).

state is a direct product of plaquette-singlets $|\psi_a\rangle$ [see Fig. 2(a)], which is defined as

$$|\psi_a\rangle = [(1, 1), (2, 2)] \otimes [(1, 2), (2, 1)] \otimes [(3, 1), (4, 2)] \otimes [(3, 2), (4, 1)] \otimes \dots \quad (3)$$

Here we have introduced a singlet at two sites $\vec{\alpha}$ and $\vec{\beta}$, $[\vec{\alpha}, \vec{\beta}] = [(\alpha_x, \alpha_y), (\beta_x, \beta_y)]$ as

$$[\vec{\alpha}, \vec{\beta}] = \frac{1}{\sqrt{2}} (|\uparrow\rangle_{\vec{\alpha}} |\downarrow\rangle_{\vec{\beta}} - |\uparrow\rangle_{\vec{\beta}} |\downarrow\rangle_{\vec{\alpha}}) \quad (4)$$

By taking into account of the translational invariance, we consider the linear combination of $|\psi_a\rangle$ and $|\psi_b\rangle$ as shown in Fig. 2(b). State $|\psi_b\rangle$ is defined as

$$|\psi_b\rangle = [(2, 1), (3, 2)] \otimes [(2, 2), (3, 1)] \otimes [(4, 1), (5, 2)] \otimes [(4, 2), (5, 1)] \otimes \dots \quad (5)$$

Notice that the two dimerized plaquette singlet states $|\psi_a\rangle$ and $|\psi_b\rangle$ are not orthogonal to each other, but their overlap is exponentially small for large N . For $N/2$ being even, the overlap is obtained as $\langle \psi_a | \psi_b \rangle = 2^{-N/2}$. As described later, the state $|\psi_s\rangle \propto |\psi_a\rangle + |\psi_b\rangle$ can be a good trial state to understand the edge states and the entanglement entropy for the vector chirality state³¹.

In the VC phase, the bulk itself has a finite gap in the thermodynamic limit^{21,24}. We introduce two types of boundaries —(a) diagonal-edge and (b) vertical-edge (see Fig. 3)³². We diagonalized the Hamiltonian numerical by the Lanczos method. In Fig. 4 we show the size dependence on the energy gap of the total $S^z = 0$ sector for $\theta = 4\pi/5$, where the bulk spin gap is relatively large. The system with the vertical-edges has almost the same excitation energy as that of the periodic one. In contrast, there exist additional low energy excited states with an exponentially small energy gap when the system has the diagonal-edges. The appearance of such a localized mode indicates the feature of the *bulk-edge correspondence*. In fact, this mode is a triplet excitation and can be interpreted as the Kennedy triplet (see Fig. 5) — triplet excitation between the effective boundary spins at both sides¹⁸. We confirmed that this mode is really a triplet excitation from the diagonalization on the different S^z sector. This mode is observed also in the different

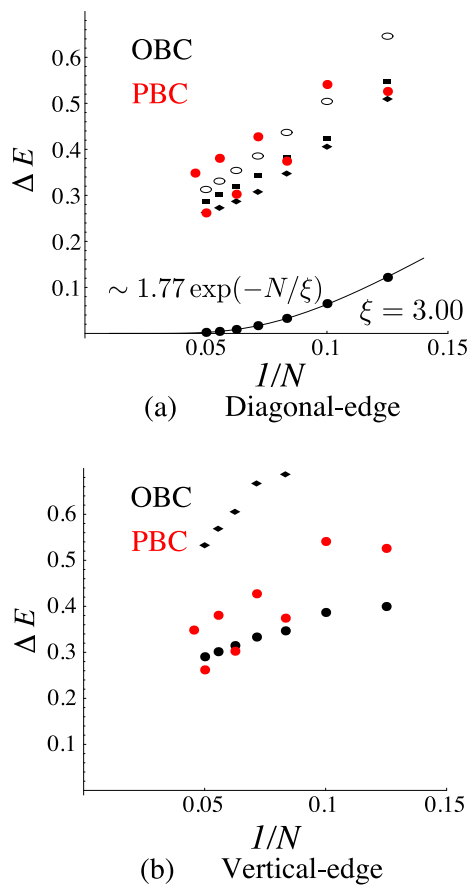


FIG. 4: System-size dependence of low excitation energy for $\theta = 4\pi/5$ with the two OBCs compared with the energy gap under the periodic boundary condition (PBC).

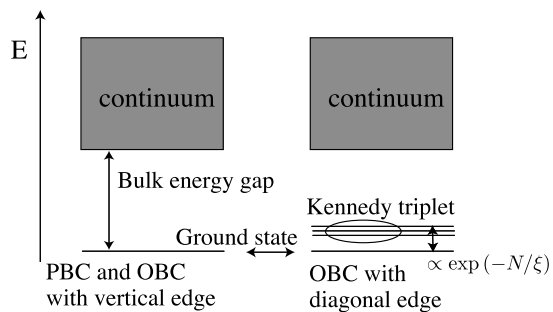


FIG. 5: Schematic picture of the low energy excitations.

(J, K) 's in VC phase³³. Note that the Kennedy triplet in this model was also discussed in a different context before²⁷.

When we introduce the boundary for the trial state $|\psi_s\rangle$, i.e., the linear combination of the two dimerized plaquette singlets, the isolated spins appear near the boundaries (see Fig. 6). In the system with diagonal-edges they appear at each boundary, while in the system

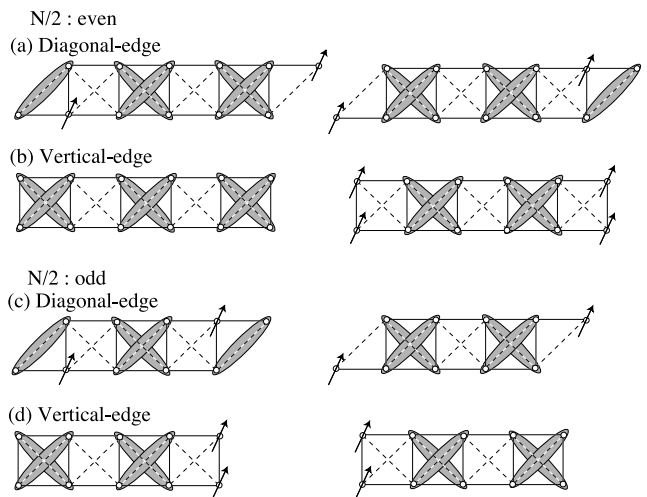


FIG. 6: Linear combination of the dimerized plaquette-singlets $|\psi_s\rangle$ with OBCs.

with vertical-edges they appear as a pair at one side of the edge. Although a pair of localized spins behaves freely in the decoupled vector chiral model \mathcal{H}_{dcv} , the pair of the spins couples each other in the original model \mathcal{H}_{cvc} with vertical-edges. Therefore, the Kennedy triplet excitation does not appear in the system with the vertical-edges. Thus the trial state $|\psi_s\rangle$ gives consistent understanding for the low energy spectra of the VC phase.

Next we consider the RS phase. In Fig. 7, we show the size dependence on the energy gap of the total $S^z = 0$ sector for $\theta = -\pi/5$. Combining with the calculation on different S^z sector we obtain the Kennedy triplet mode as in the VC phase in the case with diagonal-edge. This is consistent with the naive picture of the rung singlet, which is obtained by the Berry phase (see Fig. 8). This mode is confirmed also in the different (J, K) 's in the RS phase.

IV. ENTANGLEMENT ENTROPY

In this section, let us consider entanglement entropy for the VC state. Define the density matrix of the state $|\psi\rangle$ as $\hat{\rho} = |\psi\rangle\langle\psi|$ and divide the system into two subsystems A and B [see Figs. 9(a) and 9(b)]. Then the entanglement entropy is defined as³⁰

$$\text{E.E.} = -\langle \log \hat{\rho}_A \rangle_A = -\text{Tr} [\hat{\rho}_A \log \hat{\rho}_A].$$

Here the reduced density matrix $\hat{\rho}_A$ is given as $\hat{\rho}_A = \text{Tr}_B \hat{\rho}$. It represents how much state $|\psi\rangle$ is entangled between subsystems A and B .

Let us assume state $|\psi\rangle$ as a unique ground state under the PBC in the VC state. We take subsystem A as the subsystem with the diagonal (vertical) edges with N' spins by the reduction from $N = 20$ spin system with the PBC. Similarly as for the energy gap we consider

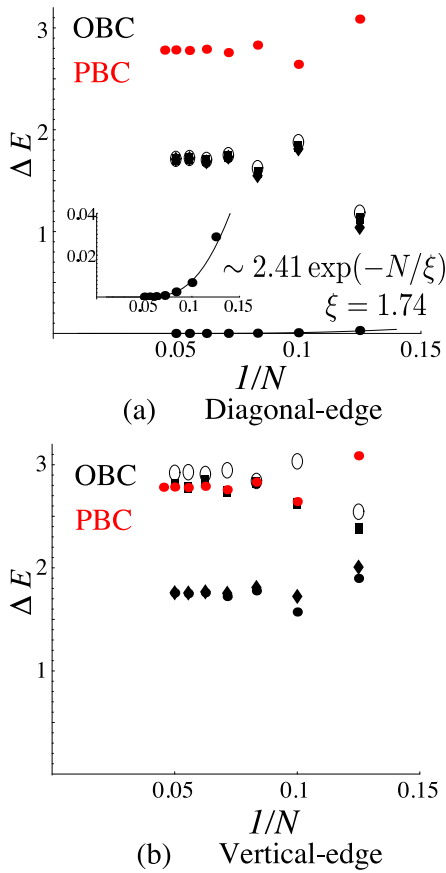


FIG. 7: System-size dependence of low excitation energy for $\theta = -\pi/5$ with the two OBCs compared with the energy gap under the periodic boundary condition (PBC). The inset is the extended figure for the first excitation state energy.

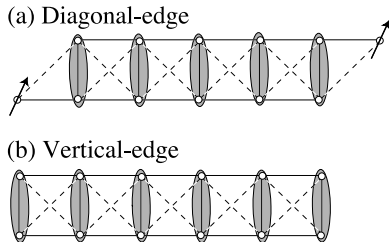


FIG. 8: Rung-singlets with OBCs.

two types of open boundaries, we calculate the entanglement entropy numerically for the cases with vertical-edge and diagonal-edge as shown in Figs. 9(a) and 9(b). Figure 9(c) shows the N' dependence of the entanglement entropy. In both cases, the obtained E.E. contains a contribution around $3 \log 2$. The contribution $3 \log 2$ can be understood by the trial state $|\psi_s\rangle$ (see the Appendix).

In the naive picture, in the RS phase the isolated single on the rung is a good trial state. Therefore we expect that $E.E. = 2 \log 2$ for the diagonal edge and that $E.E.$

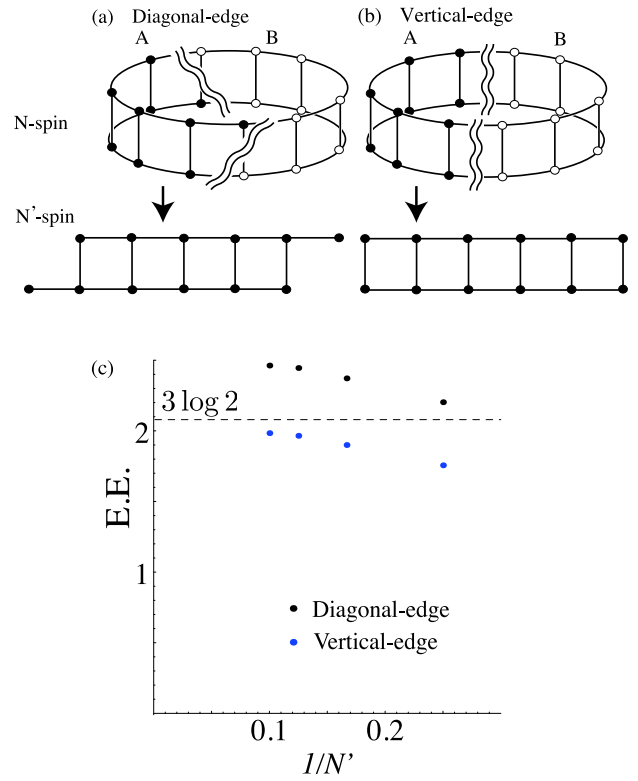


FIG. 9: Two types of the reduction to the subsystem A with (a) diagonal-edge and (b) vertical-edge. (c) Entanglement entropy of subsystem for $\theta = 4\pi/5$ with N' spins by reduction from $N = 20$ spin system.

$= 0$ for the vertical edge. We have qualitative agreement that the E.E. for the diagonal edge is larger than that for the vertical edge, although there is strong θ -dependence and large deviation from the $2 \log 2$. This is due to the relatively large overlap on the leg-direction.

V. SUMMARY

In summary, it has been shown that in the vector chirality state the dimerized plaquette singlet state $|\psi_s\rangle$ can be a good trial state to understand the numerical results for the topological properties — the edge states and the entanglement entropy. The entanglement entropy of $|\psi_s\rangle$ has been obtained as $3 \log 2$ for both types of the reduced systems while the appearance of the edge states depends on the type of boundaries. These *boundary-dependent* low energy excitations as the generic edge states characterize the vector chirality phase. This boundary dependent edge state is also observed in the rung-singlet phase. Such localized modes in the boundary are expected to be observed experimentally through the impurity or surface effect.

The work was supported in part by Grants-in-Aid for Scientific Research, Grant No.20654034 from JSPS

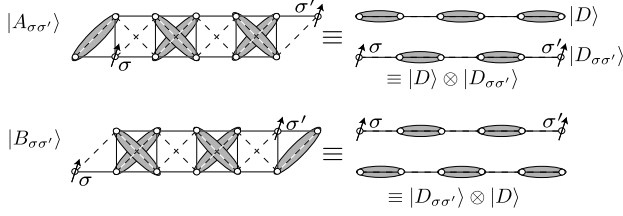


FIG. 10: Two types of the tensor products of the two dimerized states in Eq. (A6) with diagonal-edges for even $N'/2$ case ($N' = 12$), which corresponds to Fig.6 (a).

and No.220029004 (Physics of New Quantum Phases in Super-clean Materials) and No.20046002 (Novel States of Matter Induced by Frustration) on Priority Areas from MEXT (Japan). The work of YH was also supported in part by the National Science Foundation under Grant No. PHY05-51164. Some numerical calculations were carried out on Altix3700BX2 at YITP in Kyoto University and the facilities of the Supercomputer Center, Institute for Solid State Physics, University of Tokyo.

APPENDIX A: ENTANGLEMENT ENTROPY FOR THE TRIAL STATE

For example, we calculate the entanglement entropy of $|\psi_s\rangle$ in the diagonal-edge case for even $N/2$ and $N'/2$ cases. The reduced density matrix $\hat{\rho}_A$ can be obtained as (see Fig. 10),

$$\hat{\rho}_A = \frac{1}{4m} \sum_{\sigma, \sigma' = \uparrow, \downarrow} [|A_{\sigma\sigma'}\rangle\langle A_{\sigma\sigma'}| + |B_{\sigma\sigma'}\rangle\langle B_{\sigma\sigma'}|] + \frac{m'}{4m} [|A_{\uparrow\downarrow}\rangle\langle B_{\uparrow\downarrow}| - |A_{\uparrow\downarrow}\rangle\langle B_{\downarrow\uparrow}| + (A \leftrightarrow B)] \quad (\text{A1})$$

where $m = 2 + 2^{3-N/2}$ and $m' = 2^{1-(N-N')/2}$. States $|A_{\sigma\sigma'}\rangle$ and $|B_{\sigma\sigma'}\rangle$ are represented as the tensor product of the dimerized states in the zigzag chains (see Fig. 10),

$$\begin{aligned} |A_{\sigma\sigma'}\rangle &= [(1, 1), (2, 2)] \otimes |\sigma\rangle_{(2,1)} \\ &\otimes [(3, 1), (4, 2)] \otimes [(3, 2), (4, 1)] \otimes \dots \\ &\otimes [(N'/2 - 1, 1), (N'/2, 2)] \\ &\otimes [(N'/2 - 1, 2), (N'/2, 1)] \otimes |\sigma'\rangle_{(N'/2+1,2)}, \end{aligned} \quad (\text{A2})$$

$$\begin{aligned} |B_{\sigma\sigma'}\rangle &= |\sigma\rangle_{(2,1)} \otimes [(2, 1), (3, 2)] \otimes [(2, 2), (3, 1)] \otimes \dots \\ &\otimes [(N'/2 - 2, 1), (N'/2 - 1, 2)] \\ &\otimes [(N'/2 - 2, 2), (N'/2 - 1, 1)] \otimes |\sigma'\rangle_{(N'/2,2)} \\ &\otimes [(N'/2, 1), (N'/2 + 1, 2)]. \end{aligned} \quad (\text{A3})$$

We introduce the dimerized states $|D\rangle$ and $|D_{\sigma\sigma'}\rangle$ on the chain with length $N'/2$,

$$\begin{aligned} |D\rangle &= [1, 2] \otimes [3, 4] \otimes \dots \otimes [N'/2 - 1, N'/2], \quad (\text{A4}) \\ |D\rangle_{\sigma\sigma'} &= |\sigma\rangle_1 \otimes [2, 3] \otimes \dots \\ &\otimes [N'/2 - 2, N'/2 - 1] \otimes |\sigma'\rangle_{N'/2}. \end{aligned} \quad (\text{A5})$$

Changing site indexes to decouple the ladder into two chains, we have equivalences $|A_{\sigma\sigma'}\rangle = |D\rangle \otimes |D\rangle_{\sigma\sigma'}$ and $|B_{\sigma\sigma'}\rangle = |D\rangle_{\sigma\sigma'} \otimes |D\rangle$ (see Fig. 10). Here we have introduced the normalized state $|\tilde{D}\rangle \propto |D\rangle - \langle D_{\uparrow\downarrow}|D\rangle|D_{\uparrow\downarrow}\rangle - \langle D_{\downarrow\uparrow}|D\rangle|D_{\downarrow\uparrow}\rangle$ by the Gram-Schmidt orthogonalization method. Then we have the following relation:

$$\hat{\rho}_A \simeq \frac{1}{8} \sum_{\sigma, \sigma' = \uparrow, \downarrow} \left[(|\tilde{D}\rangle \otimes |D_{\sigma\sigma'}\rangle) \left(\langle \tilde{D}| \otimes \langle D_{\sigma\sigma'}| \right) + (|D_{\sigma\sigma'}\rangle \otimes |\tilde{D}\rangle) \left(\langle D_{\sigma\sigma'}| \otimes \langle \tilde{D}| \right) \right], \quad (\text{A6})$$

The approximation holds up to the order $\mathcal{O}(2^{-N'/2}) + \mathcal{O}(2^{-(N-N')/2})$ and the eight summands correspond to the states shown in Fig. 6(a). Thus, the entanglement entropy is obtained as E.E. $\simeq -8 \times \frac{1}{8} \log \frac{1}{8} = 3 \log 2$. In a similar manner we can calculate the entanglement entropy in the case of the other geometry. The entanglement entropy counts the degrees of freedom of the spins around the edges, although the Kennedy triplet does not appear in the system with vertical-edge due to the short range residual interaction between the localized effective spins.

¹ F.D.M. Haldane, Phys. Lett. A **93**, 464 (1983).

² I. Affleck, T. Kennedy, E. H. Lieb, and H. Tasaki, Phys.

- Rev. Lett. **59**, 799 (1987).
- ³ D.P. Arovas, A. Auerbach, and F.D.M. Haldane, Phys. Rev. Lett. **60**, 531 (1988).
 - ⁴ H. Katsura, T. Hirano, and Y. Hatsugai, Phys. Rev. B **76**, 012401 (2007).
 - ⁵ A. Kitaev, and J. Preskill, Phys. Rev. Lett. **96**, 110404 (2006).
 - ⁶ M. Levin, and X.G. Wen, Phys. Rev. Lett. **96**, 110405 (2006).
 - ⁷ E. H. Lieb, T. Schultz, and D. J. Mattis, Ann. Phys. (N.Y.) **16**, 407 (1961).
 - ⁸ Y. Hatsugai, J. Phys. Soc. Jpn. **73**, 2604 (2004); **74**, 1374 (2005); **75**, 123601 (2006).
 - ⁹ T. Hirano, H. Katsura, and Y. Hatsugai, Phys. Rev. B **77**, 094431 (2008); Phys. Rev. B **78**, 054431 (2008).
 - ¹⁰ X.G. Wen, Phys. Rev. B **40**, 7387 (1989).
 - ¹¹ R.B. Laughlin, Phys. Rev. B **23**, 5632 (1981).
 - ¹² B. I. Halperin, Phys. Rev. B **25**, 2185 (1982).
 - ¹³ Y. Hatsugai, Phys. Rev. Lett. **71**, 3697 (1993).
 - ¹⁴ Y. Hatsugai, Phys. Rev. B **48**, 11851 (1993).
 - ¹⁵ Y. Hatsugai, T. Fukui, and H. Aoki, Phys. Rev. B **74**, 205414 (2006).
 - ¹⁶ M. Arikawa, Y. Hatsugai, and H. Aoki, Phys. Rev. B **78**, 205401 (2008).
 - ¹⁷ Y. Hatsugai, arXiv:0811.1633, to appear in Solid State Communications (2009).
 - ¹⁸ T. Kennedy, J.Phys: Condens. Matter **2**, 5737 (1990).
 - ¹⁹ M. Hagiwara, K. Katsumata, I. Affleck, B. I. Halperin, and J. P. Renard, Phys. Rev. Lett. **65**, 3181 (1990).
 - ²⁰ T. Hirano, and Y. Hatsugai, J. Phys. Soc. Jpn. **76**, 074603 (2007).
 - ²¹ A. Läuchli, G. Schmid, and M. Troyer, Phys. Rev. B **67**, 100409(R) (2003).
 - ²² Y. Honda, Y. Kuramoto, and T. Watanabe, Phys. Rev. B **47**, 11329 (1993).
 - ²³ K.P. Schmidt, H. Monien, and G.S. Uhrig, Phys. Rev. B **67**, 184413 (2003).
 - ²⁴ T. Hikiyama, T. Momoi, and X. Hu, Phys. Rev. Lett. **90**, 087204 (2003).
 - ²⁵ N. Haga, and S. Suga, Phys. Rev. B **66**, 132415 (2002).
 - ²⁶ S. Nishimoto, and M. Arikawa, Phys. Rev. B **79**, 113106 (2009).
 - ²⁷ K. Hijii, S. Qin, and K. Nomura, Phys. Rev. B **68**, 134403 (2003).
 - ²⁸ J.L. Song, S.J. Gu, and H.Q. Lin, Phys. Rev. B **74**, 155119 (2006).
 - ²⁹ I. Maruyama, T. Hirano, and Y. Hatsugai, Phys. Rev. B **79**, 115107 (2009); J. Phys. Conf. Ser. **145** 012052 (2009).
 - ³⁰ G. Vidal, J. I. Latorre, E. Rico, and A. Kitaev, Phys. Rev. Lett. **90**, 227902 (2003).
 - ³¹ The phase factor can be arbitrary on $|\psi_b\rangle$.
 - ³² We make a boundary by truncating all terms $\mathbf{S}_i \cdot \mathbf{S}_j$ and $(\mathbf{S}_i \cdot \mathbf{S}_j)(\mathbf{S}_k \cdot \mathbf{S}_l)$ whose bond cross the boundary. Note that some terms of $P_x + P_x^{-1}$ in Eq. (2) do not cross the boundary even in the vertical-edge case.
 - ³³ Close to the phase boundary, the correlation length becomes large and the bulk spin gap is very tiny. In this case, "Kennedy triplet" is hardly observed.